POLITECNICO DI TORINO
Repository ISTITUZIONALE

Vibration of metallic and composite shells in geometrical nonlinear equilibrium states

(Article begins on next page)

18 October 2022

Vibration of metallic and composite shells in geometrical nonlinear equilibrium states

E. Carrera,[*] A. Pagani,[†] R. Azzara,[‡] R. Augello [§]

Mul^2 group

Department of Mechanical and Aerospace Engineering, Politecnico di Torino
Corso Duca degli Abruzzi 24, 10129 Torino, Italy

Abstract: *By making use of high order shell models, the present work discusses frequency and mode change of thin structures subjected to large displacements and rotations. The models are implemented in the domain of the well-established Carrera Unified Formulation (CUF) and employ the full Green-Lagrange strain tensor, in a total Lagrangian scenario. In this manner, finite elements to be applied indistinctively to metallic and laminated composite shells, having refined layerwise kinematics, and providing accurate nonlinear equilibrium states as well as vibration analysis in both moderate and large displacement fields are provided. Several numerical examples are discussed for shell problems dominated by flexure and compression. The validity of the proposed formulation is demonstrated and modal aberrations as a consequence of the loading, the nonlinear equilibrium state, and the material anisotropy is discussed.*

Keywords: Carrera Unified Formulation; Nonlinear vibration; Refined 2D shell theory; Geometrical nonlinearity; Mode aberration.

1   Introduction

The extensive use of thin-walled elements in the design and fabrication of a large number of engineering structures, especially in aerospace, has attracted the interest of many researchers in the last few decades. Shell structures are widely investigated by researchers and scientists for their excellent characteristics. In fact, these structures are capable of supporting external loads with high efficiency and of undergoing large displacements and rotations when external loads become extreme.

The reliability of these isotropic and composite structures depends directly on their performances. Consequently, investigations on the dynamic behaviours of these components are crucial in the design and verification of structures, particularly for aeronautical and space applications. During their service life, large amplitude vibrations are widely present in thin-walled structures. Moreover, considerable states of pre-stress within the structure can be present as a consequence of large displacements and rotations. When a vibrating structure exhibits large amplitudes, it is appropriate to include geometrical nonlinearities in order to perform accurate dynamic analyses [1]. As reported by Chen and Babcock [2], two phenomena describe in detail the nonlinear effects of large amplitude vibration on cylindrical shell structures; the response-frequency relations in the vicinity of a resonant frequency and the occurrence of travelling wave response. In contrast to the linear vibrations, the resonant frequency in nonlinear vibrations depends on its amplitude vibration. The hardening-type (frequency increasing with amplitude) and softening-type (frequency decreasing with amplitude) represent the two different nonlinearities in the response-frequency relationship.

---

[*]Professor of Aerospace Structures and Aeroelasticity. E-mail: erasmo.carrera@polito.it
[†]Associate professor. E-mail: alfonso.pagani@polito.it
[‡]PhD student. E-mail: rodolfo.azzara@polito.it
[§]PhD student. E-mail: riccardo.augello@polito.it

The evaluation of natural frequencies and relative mode shapes is immensely useful in structural analysis. In fact, many works on the procedure for calculating the natural frequencies of a structure are available in the literature. As an example, Wittrick and Williams [3] proposed a general algorithm for determining the natural frequencies of elastic structures. The same authors [4] implemented a theory for performing vibration analysis to compute the natural frequencies of isotropic or anisotropic 2D structure subjected to combined loadings. Virgin [5] provided a complete description of the vibration analysis of slender structural components under compressive loadings. Since the modal behaviour of the structure is a property of the equilibrium state condition and pre-stress within the structure, the natural frequencies and the relative mode shapes undergo changes due to the presence of nonlinear effects. As an example, Amabili and Païdoussis [6] provided a detailed review of works on the geometrical nonlinear vibrations and dynamic response of shells. Biot [7] implemented a nonlinear formulation of elasticity, considering first and second-order terms, to write the kinematic relations, and he studied the linearized case for a structure with initial stress, showing the considerable effect on the equilibrium and vibrations. In recent years, the open literature has shown a great interest from researchers and scientists about this topic. In fact, a large number of works on large amplitude vibration of cylindrical shells are available. Similar evaluations are found in the paper of Hermann [8], Odgen and Roxburgh [9], and Abkarov [10], where a review of analyses on the study of the dynamic properties of isotropic structures with pre-stress conditions is carried out. Instead, the same analysis, but considering a composite plate with initial stresses, was performed by Sun and Whitney [11].

In the field of mechanics, shell are the most common structures in practical applications. Their dynamic properties are of great interest to designers in order to improve performances. In the context of nonlinear vibration analysis, a comprehensive review of vibration shell theories was done by Leissa [12]. Many other authors studied the nonlinear free vibration analysis to evaluate the dynamic behaviour of structures. As an example, Shin [13] adopted the first-order shear deformation theory (FSDT) and von Kàrmàn geometric nonlinearities to study the behaviour of composite shells under large amplitude vibrations. The hardening-type nonlinearity in free flexural vibration of cylindrical shells was considered for isotropic shells by Chu [14] and for orthotropic shells by Nowinski [15]. In contrast, Olson [16], Mayers and Wrenn [17] and Evensen and Fulton [18] performed nonlinear vibration analysis using a softening nonlinearity. The finite element method to study nonlinear free vibrations of single/doubly curved laminated shallow shell was employed by Singh and Panda [19]. Large amplitude vibrations of anisotropic cylindrical shell structures using a semi-analytical method were described by Toorani and Lakis [20]. An eight-noded C^0 continuity isoparametric quadrilateral element was introduced by Nanda and Bandyopadhyay [21] to evaluate the nonlinear free vibration analysis of composite shells with cutouts. A significant review of different approaches for studying the vibration analysis of plates and shells in both linear and nonlinear domains was reported by Banerjee and Mazumdar [22]. Recently, a semi-analytical formulation based on Lagrange's equations was used by Rougui *et al.* [23] to perform geometrical nonlinear free and forced vibrations of simply supported shells. The effect of large displacements on the linearized vibration of composite structures was performed by Carrera *et al.* [24]. Pagani *et al.* [25] evaluated the frequency and mode change in the large deflections and post-buckling of compact and thin-walled structures.

The goal of the present paper is to propose an approach to investigate nonlinear vibration characteristics of shells. Thus, the change of natural frequency and relative mode shapes in the case of large deformation of isotropic and composite shell structures is analyzed. A similar approach is adopted in real applications, see Abramovich *et al.* [26], Arbelo *et al.* [27] and Lurie [28], both to measure experimentally the natural frequencies of a loaded structure and to monitor their change for progressively increasing loads. This methodology, known as Vibration Correlation Technique (VCT), is a non-destructive and experimental approach for computing the buckling condition, by interpolating the natural frequencies of the structure at progressive loadings, without reaching the instability point within the tested structure. A detailed description of this method is not the scope of this article; readers are referred to [29, 30] for more details.

The proposed nonlinear approach is formulated in the domain of the Carrera Unified Formulation (CUF) [31, 32]. CUF represents a hierarchical formulation in which the order of the structural model is considered as an input of the analysis. Thus, no ad-hoc formulations are needed to achieve any refined generic model. As reported by Carrera *et al.* [33], any theory is degenerated into generalized kinematics using arbitrary expansions. With this procedure, it is possible to express the nonlinear governing equations and the relative Finite Element (FE) arrays of the shell formulations in terms of *Fundamental Nuclei* (FNs). FNs are the basic building blocks of the proposed formulation. CUF was adopted in different engineering applications [34, 35, 36, 37], and it was, recently, extended to nonlinear geometric analysis for the resolution of metallic and composite models [38, 39, 40, 41].

The present manuscript is structured as follows: (i) first, some important aspects regarding the notation of the two-dimensional (2D) shell CUF model, including the Green-Lagrange nonlinear geometrical relations, are illustrated in Section 2; (ii) then, Section 3 briefly shows the linearized eigenvalue problem solved to evaluate the mode change. Furthermore, it describes the methodology applied in the present paper to investigate the natural frequencies; (iii) next, Section 4 reports and discusses numerical results for different shell structures and loadings; (iv) finally, Section 5 outlines the conclusions.

2 Carrera Unified Formulation (CUF)

A shell structure, which is represented employing an orthogonal curvilinear reference system (α, β, z), where α and β denote the two in-plane directions and z the through-the-thickness direction, is shown in Fig 1. For the sake of clarity, the following discussion is done considering a composite material,
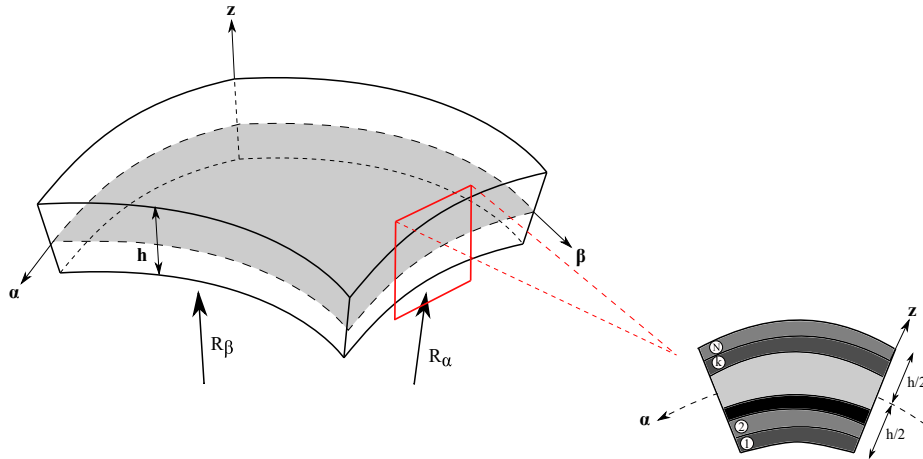

Figure 1: Geometry and reference system of a generic doubly-curve shell model.

in which k indicates the kth layer, see Fig. 1. With no loss of generality, the same formulation can be simplified for homogeneous metallic structures.

The transposed displacement vector is written as follows:

$$\boldsymbol{u}^k(\alpha, \beta, z) = \{ \ u_\alpha^k \ u_\beta^k \ u_z^k \ \}^T \tag{1}$$

The strain, $\boldsymbol{\epsilon}$, and stress, $\boldsymbol{\sigma}$, for each layer k are formulated as:

$$\boldsymbol{\epsilon}^k = \{\epsilon_{\alpha\alpha}^k, \ \epsilon_{\beta\beta}^k, \ \epsilon_{zz}^k, \ \epsilon_{\alpha z}^k, \ \epsilon_{\beta z}^k, \ \epsilon_{\alpha\beta}^k\}^T$$

$$\boldsymbol{\sigma}^k = \{\sigma_{\alpha\alpha}^k, \ \sigma_{\beta\beta}^k, \ \sigma_{zz}^k, \ \sigma_{\alpha z}^k, \ \sigma_{\beta z}^k, \ \sigma_{\alpha\beta}^k\}^T \tag{2}$$

When dealing with large displacements of flexible structures, the Green-Lagrange nonlinear strains are assumed. Hence, the strain vector $\boldsymbol{\epsilon}^k$ can be related to displacement components as:

$$\boldsymbol{\epsilon}^k = \boldsymbol{\epsilon}_l^k + \boldsymbol{\epsilon}_{nl}^k = (\boldsymbol{b}_l + \boldsymbol{b}_{nl})\boldsymbol{u}^k \tag{3}$$

where $\boldsymbol{b}_l$ and $\boldsymbol{b}_{nl}$ represent the linear and nonlinear differential operators, respectively. These differential operators in the case of the 2D shell models are reported in [33]. In this paper, both isotropic and composite shells are analyzed. Hence, using the constitutive equations the stresses are computed as:

$$\boldsymbol{\sigma}^k = \tilde{\boldsymbol{C}}^k \boldsymbol{\epsilon}^k \tag{4}$$

where the material elastic matrix $\tilde{\boldsymbol{C}}$ can be found in [42, 43].

According to the CUF, the three-dimensional (3D) displacement field $\boldsymbol{u}(\alpha, \beta, z)$ is written in the compact form as shown in Eq. (5):

$$\boldsymbol{u}^k(\alpha, \beta, z) = F_\tau^k(z)\boldsymbol{u}_\tau^k(\alpha, \beta) \qquad \tau = 0, 1, ..., N \tag{5}$$

where $\boldsymbol{u}_\tau(\alpha, \beta)$ indicates the generalized in-plane displacement vector, F_τ represents the expansion functions of the thickness coordinate z, k indicates the layer index and N denotes the order of the expansion in the thickness direction. The choice of F_τ and N is arbitrary and determines the class of the considered 2D CUF shell model. Readers are referred to [32] for the complete mathematical derivation of shell FE formulations in the domain of CUF. In the present work, the adopted shell theories are denoted by the acronym LDN, which represent the Lagrange Expansion (LE), Displacement-based theory with the order N. In particular, the four-node cubic (LD3) Lagrange expansion functions are assumed in the z-direction in order to generate a high order kinematics CUF shell models with geometrical nonlinearity. As for the composite models, the layerwise (LW) approach adopting LE is considered.

Independently of the selected shell model kinematics, the Finite Element Method (FEM) is adopted to approximate the in-plane generalized displacement vector using the shape functions $N_i(\alpha, \beta)$.

$$\boldsymbol{u}_\tau^k(\alpha, \beta) = N_i(\alpha, \beta)\boldsymbol{q}_{\tau i}^k \qquad i = 1, 2, ..., n_{el} \tag{6}$$

where $\boldsymbol{q}_{\tau i}$ are the unknown nodal variables, n_{el} represents the number of nodes per element and the i indicates summation. Furthermore, using CUF and introducing FEM, the strain vector is formulated in algebraic form as:

$$\boldsymbol{\epsilon}^k = (\boldsymbol{B}_l^{\tau i} + \boldsymbol{B}_{nl}^{\tau i})\boldsymbol{q}_{\tau i}^k \tag{7}$$

where $\boldsymbol{B}_l^{\tau i}$ and $\boldsymbol{B}_{nl}^{\tau i}$ represent the linear and nonlinear algebraic matrices. The complete formulation of these matrices can be found in [39].

In the following analyses, the classical 2D nine-node quadratic FE (Q9) is considered for the shape function in the α-β plane. For the sake of completeness, Fig. 2 shows the approximations for a typical shell structure, with the different modelling for isotropic and composite structures: 1LD2 for the isotropic and 3LD2 (1LD2 for each layer) for the composite, respectively. In the first case, we consider a through-the-thickness quadratic model for the analysis of the metallic shell structure. In the latter case, a piece-wise quadratic LW model is assumed for the composite.

3 Nonlinear free vibration of shell structures

The equations of motion of a structure undergoing undamped free vibrations are derived using the principle of virtual work. It reads:

$$\delta L_{int} = -\delta L_{ine} \tag{8}$$

where δL_{int} and δL_{ine} represent the virtual variation of the strain energy and the virtual variation of the inertia loads, respectively. Substituting Eq. (7) and the constitutive relations for elastic materials (Eq. (4)) into Eq. (8), the virtual variation of the strain energy is written as:

$$
\begin{aligned}
\delta L_{int} &= \delta \boldsymbol{q}_{sj}^T \boldsymbol{K}_0^{ij\tau s} \boldsymbol{q}_{\tau i} + \delta \boldsymbol{q}_{sj}^T \boldsymbol{K}_{lnl}^{ij\tau s} \boldsymbol{q}_{\tau i} + \delta \boldsymbol{q}_{sj}^T \boldsymbol{K}_{nll}^{ij\tau s} \boldsymbol{q}_{\tau i} + \delta \boldsymbol{q}_{sj}^T \boldsymbol{K}_{nlnl}^{ij\tau s} \boldsymbol{q}_{\tau i} \\
&= \delta \boldsymbol{q}_{sj}^T \boldsymbol{K}_S^{ij\tau s} \boldsymbol{q}_{\tau i}
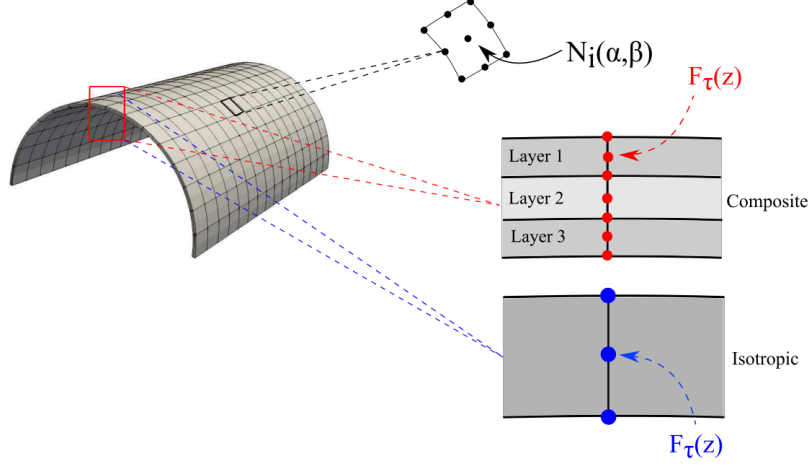\end{aligned}
\tag{9}
$$

Figure 2: FE discretization and CUF kinematics in the modelling of shells.

where $\boldsymbol{K}_S^{ij\tau s}$ is the secant stiffness matrix, $\boldsymbol{K}_0^{ij\tau s}$ is the linear contribution of $\boldsymbol{K}_S$ and $\boldsymbol{K}_{lnl}^{ij\tau s}$, $\boldsymbol{K}_{nll}^{ij\tau s}$ and $\boldsymbol{K}_{nlnl}^{ij\tau s}$ are the nonlinear components. These contributions are formulated in the form of FNs. Readers are referred to [44] for the explicit derivation of the stiffness FNs. Similarly, the FNs of the linear mass matrix is formulated from the virtual variation of the inertial loads:

$$\delta L_{ine} = \delta \boldsymbol{q}_{sj}^T \boldsymbol{M}^{ij\tau s} \ddot{\boldsymbol{q}}_{\tau i} \tag{10}$$

where $\boldsymbol{M}^{ij\tau s}$ is the FN of the mass matrix.

The analysis of free vibrations is performed around a linearized state of equilibrium along the path of equilibrium. The modal behaviour of a structure is not only a property of the geometrical and mechanical characteristics, but above all, it is a property of the state of equilibrium. Therefore, assuming the virtual variation of the inertial loads as linear, the virtual variation of the nonlinear strain energy has to be linearized to compute the tangent stiffness matrix.

$$\delta(\delta L_{int}) = \delta \boldsymbol{q}_{sj}^T (\boldsymbol{K}_0^{ij\tau s} + \boldsymbol{K}_{T1}^{ij\tau s}) \boldsymbol{q}_{\tau i} + \delta \boldsymbol{q}_{sj}^T \boldsymbol{K}_\sigma^{ij\tau s} \boldsymbol{q}_{\tau i}$$
$$= \delta \boldsymbol{q}_{sj}^T \boldsymbol{K}_T^{ij\tau s} \boldsymbol{q}_{\tau i} \tag{11}$$

where $\boldsymbol{K}_T^{ij\tau s}$ represent the FN of the tangent stiffness matrix, $\boldsymbol{K}_0^{ij\tau s}$ indicates the linear component of $\boldsymbol{K}_T$, $\boldsymbol{K}_{T1}^{ij\tau s} = 2\boldsymbol{K}_{lnl}^{ij\tau s} + \boldsymbol{K}_{nll}^{ij\tau s} + 2\boldsymbol{K}_{nlnl}^{ij\tau s}$ is the nonlinear contribution, and $\boldsymbol{K}_\sigma^{ij\tau s}$ is the the so-called *geometric stiffness*. Note that the FE matrices are expressed in terms of 3×3 FNs, which are invariant of the theory approximation order, see [32].

The resolution of this proposed method is performed as follows:

- The static geometrical nonlinear problem is solved employing the Newton-Raphson method, along with an opportune arc-length path-following constraint [45, 46];

- Given the nonlinear equilibrium curve, the tangent stiffness matrix is calculated in the states of interest, see Fig. 3;

- Assuming harmonic displacements around non-trivial equilibrium states, the equations of motion simplify into a linear eigenvalue problem from which it is possible to calculate natural frequencies and mode shapes:

$$(\boldsymbol{K}_T^{ij\tau s} - \omega^2 \boldsymbol{M}^{ij\tau s}) \boldsymbol{q}_{\tau i} = 0 \tag{12}$$

- It is important to underline how the nonlinear vibrations show low amplitudes; therefore, it is legitimate to adopt a linearization around the state of equilibrium for the resolution of the problem.
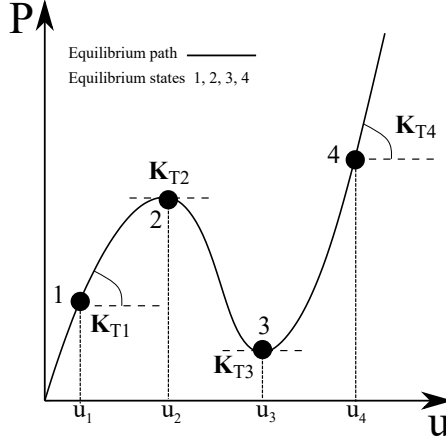
5

Figure 3: $\boldsymbol{K}_T$ at the equilibrium conditions of a nonlinear equilibrium path.

4   Numerical results

This section discusses the effect of the large displacements and rotations and pre-stress states on the natural frequencies of isotropic and composite shell structures. Moreover, the capabilities of the proposed nonlinear refined theory to detect important mode change with respect to the increased load are shown. First, the equilibrium curve for the different models is reported. It must be clarified that the displacement is measured at the load point. Then, natural frequencies, mode shapes and the Modal Assurance Criterion (MAC) values are provided. In particular, the MAC is calculated to highlight the differences between the modes of the highly deformed structure and undeformed one. Many of the problems considered represent well-known benchmark problems from [47].

4.1   Metallic and composite pinched cylindrical shell

The first analysis deals with a clamped cylindrical shell subjected to a pinching force. The vertical deflection and the rotation about the β-axis are restrained along its longitudinal edges. Besides a metallic structure, a laminate one with stacking sequence $[90°, 0°, 90°]$ is also considered. Figure 4 shows the pinched cylindrical shell under consideration. The geometrical properties of
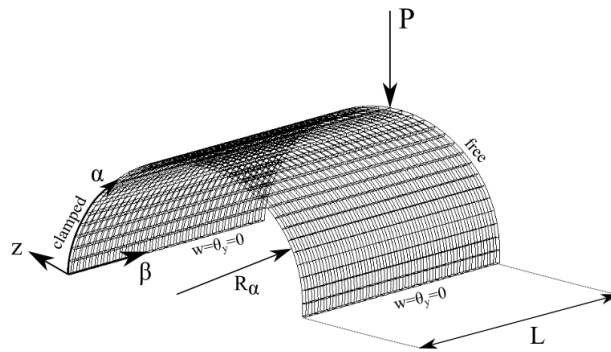

Figure 4: Pinched cylindrical shell subjected to an end pinching force.

the investigated model are: L= 3.048 m, R_α= 1.016 m, and thickness (h) equal to 0.03 m. The isotropic structure has the following material properties: E= 2.0685×10^7 N/m^2, ν= 0.3. Instead, for the composite structure the orthotropic material has Young moduli E_L= 2068.5×10^4 N/m^2, E_T= 517.125×10^4 N/m^2, shear moduli G_{LT}= 795.6×10^4 N/m^2 and Poisson's ratio ν_{LT}=ν_{TT}= 0.3. The nonlinear static behaviour of this structure was already validated in [47]. The present structure is modelled using 32×32Q9 for the in-plane mesh and one LD3 in the z-direction for the isotropic model, whereas 3LD3 kinematics is adopted for the through-the-thickness of the composite shell.

6

Figure 5 illustrates the quasi-static equilibrium curve for the studied isotropic and composite shell models. Some of the most relevant deformed configurations are also reported in the same figure. At each step of the nonlinear equilibrium curve, free vibrations are computed, adopting the local
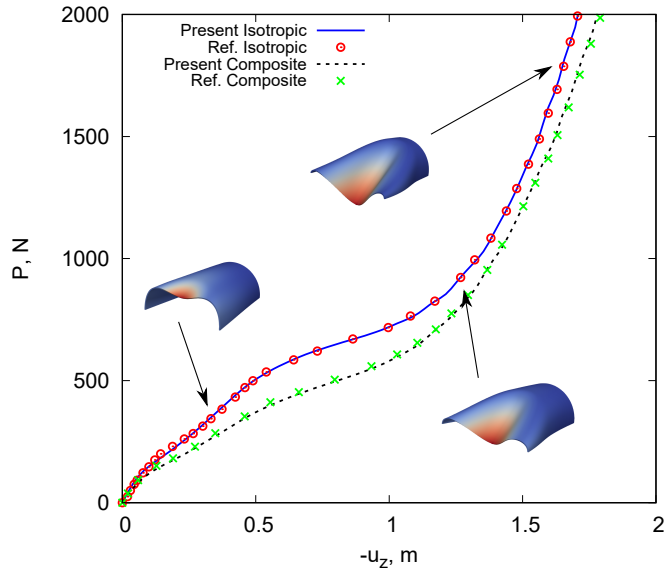

Figure 5: Equilibrium curves of the pinched isotropic and composite cylindrical shell subjected to an end pinching force.

tangent stiffness of the deformed configuration. In Table 1, the natural frequency values for the first three mode shapes as a function of the transverse displacements are shown. The values of u_z are referred to Fig. 5. Figure 6 reports the trends of the first six natural frequencies with respect to

	Isotropic				Composite		
$-u_z$	$f_1/\sqrt{\rho}$	$f_2/\sqrt{\rho}$	$f_3/\sqrt{\rho}$	$-u_z$	$f_1/\sqrt{\rho}$	$f_2/\sqrt{\rho}$	$f_3/\sqrt{\rho}$
0.00	56.82	56.55	95.44	0.00	44.05	51.77	90.76
0.24	47.59	50.32	86.43	0.13	40.78	48.38	82.61
0.57	29.99	44.38	81.90	0.63	21.16	37.75	65.98
1.11	16.89	39.11	59.14	1.12	20.41	42.85	48.93
1.36	24.43	44.54	52.44	1.46	21.13	42.04	48.06
1.48	22.68	45.23	52.63	1.58	20.77	37.84	48.39

Table 1: Natural frequencies [Hz/(kg/m^3)] for different transverse displacement [m]. Pinched isotropic and composite cylindrical shells.

the transverse displacement. It can be observed that the natural frequencies decrease as the load rises. In these plots, we underline the crossing between mode 5 and mode 6 and the interaction with mode 4 in both isotropic and composite results. Moreover, the change of these mode shapes all along the quasi-static equilibrium path of the pinched composite structure is shown in Figs. 7 and 8. The most significant MAC graphical representations are illustrated in Fig. 9. MAC is a scalar indicating correspondence between two sets of mode shapes, see [48, 49]. Different values of the nonlinear analysis are reported in comparison with the linear case ($u_z = 0$ m). The figures compare the first 10 modes for progressively increasing displacements. As reported by these graphical representations, natural modes for a low load (Fig. 9a) are identical to those related to the linear case ($u_z = 0$ m); i.e., all the MAC values in the diagonal are equal to 1. In Figs. 9b to 9d, the state is entirely nonlinear; in fact, dark boxes are all different from 1. This suggests that the structure shows
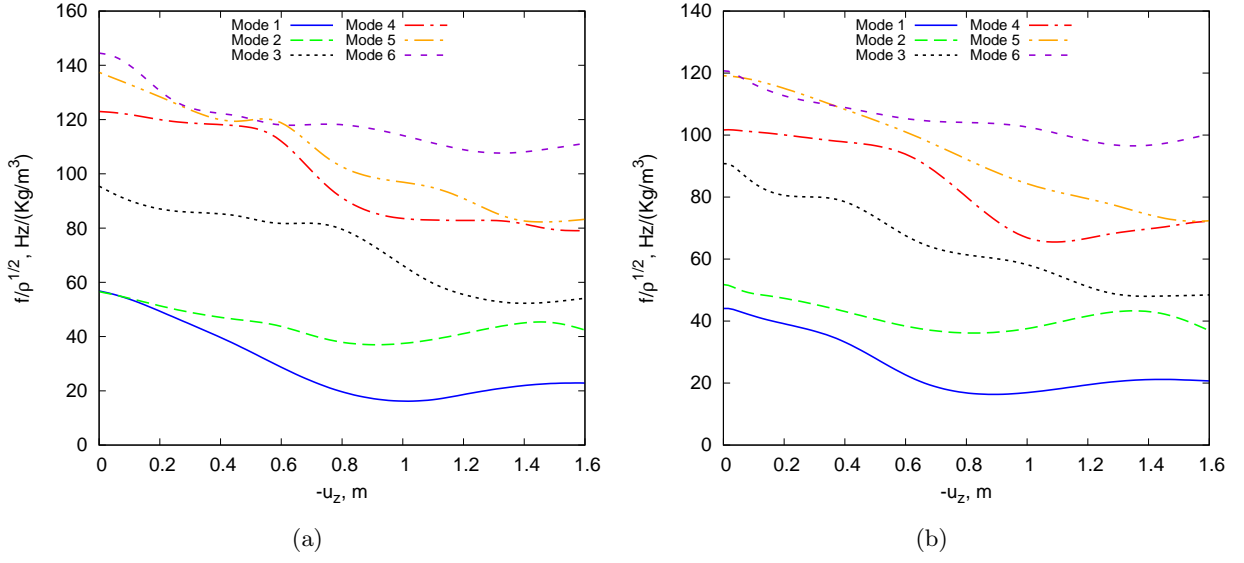
Figure 6: Natural frequencies from modes 1 to 6. Pinched isotropic (a) and composite (b) cylindrical shell subjected to an end pinching force for progressively increasing displacements.
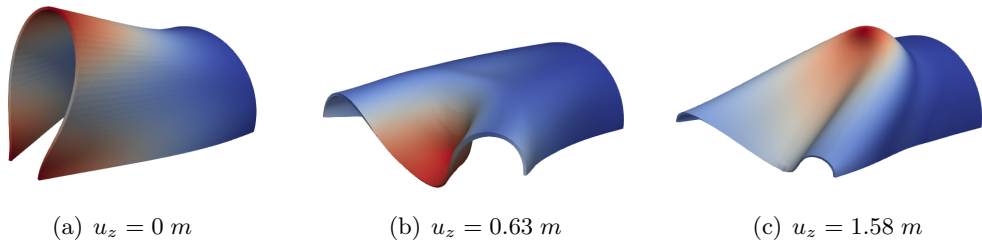

(a) $u_z = 0\ m$ (b) $u_z = 0.63\ m$ (c) $u_z = 1.58\ m$

Figure 7: First mode shape of the pinched composite cylindrical shell subjected to a pinching force for progressively increasing displacements.
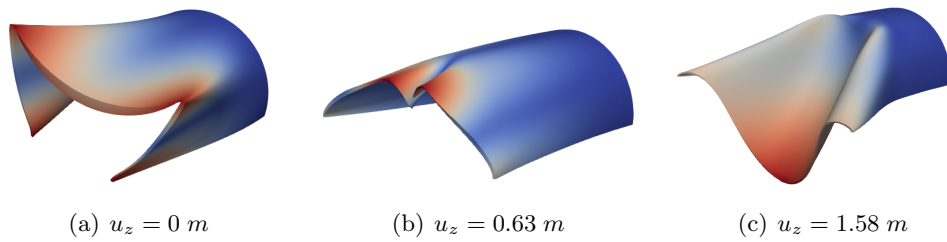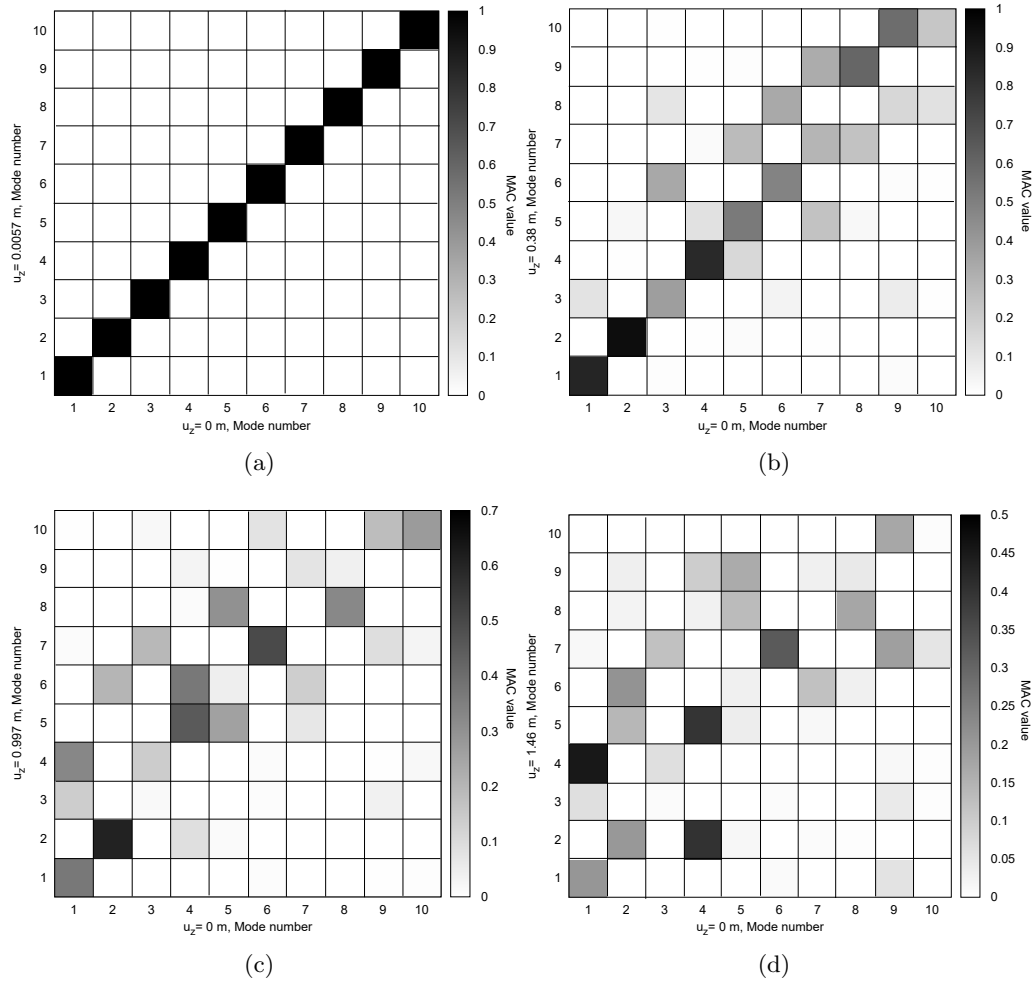

(a) $u_z = 0\ m$ (b) $u_z = 0.63\ m$ (c) $u_z = 1.58\ m$

Figure 8: Second mode shape of the pinched composite cylindrical shell subjected to a pinching force for progressively increasing displacements.

Figure 9: MAC values between the modes of the undeformed structure and those of the deformed structure for the pinched composite cylindrical shell.

a significant nonlinear influence, so the mode aberration analysis is crucial to predict the dynamic behaviours accurately.

In addition, the analysis for the pinched composite cylindrical shell subjected to compressive and transverse loads is also provided. The geometry, the constraints and the loading conditions are shown in Fig. 10a. Moreover, Fig. 10b illustrates the equilibrium curve (compressive load P_β versus transverse displacement). In this case, the compressive-transverse load ratio is equal to 66. The
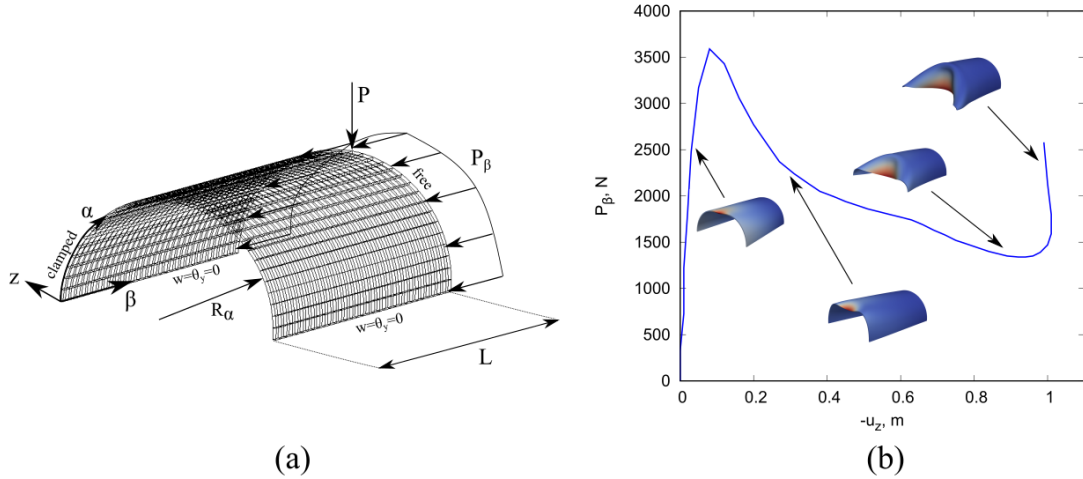
Figure 10: (a) Pinched composite cylindrical shell subjected to compressive and transverse loads. (b) Equilibrium curve at the transverse load point.

trends of the first five natural frequencies with respect to the transverse displacement is reported in Fig. 11. Figures 12 and 13 report the evolution of some important mode as a function of the quasi-
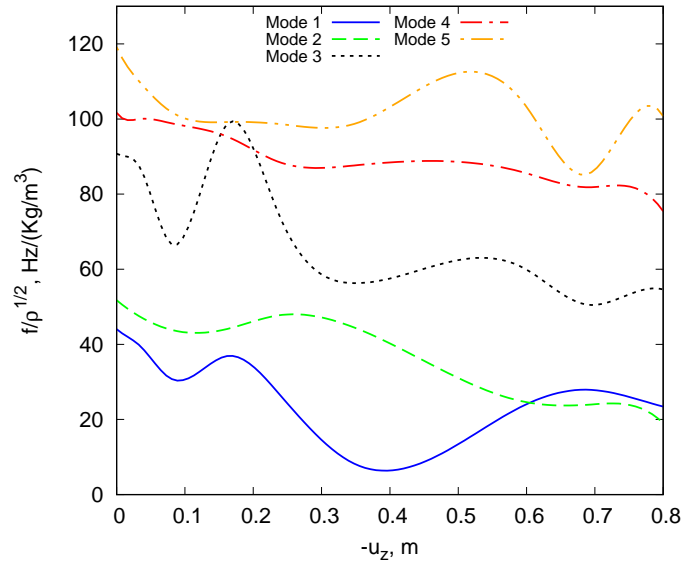

Figure 11: Natural frequencies from modes 1 to 5. Pinched composite cylindrical shell subjected to compressive and transverse loads.

static equilibrium path of the pinched composite cylindrical shell under compressive and transverse loads. Finally, the MAC graphical representations are provided in Fig. 14. From the Figs. 11, 12 and 13 it is clear that the natural frequencies and, therefore, the relative modal shapes undergo a considerable change with the progressive increase of the nonlinear quasi-static analysis. Moreover,

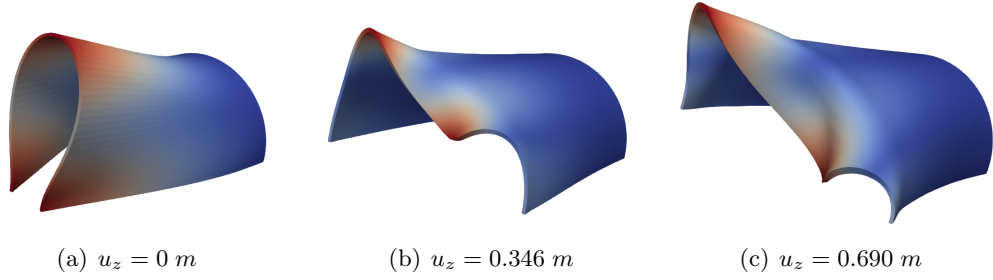(a) $u_z = 0\ m$ (b) $u_z = 0.346\ m$ (c) $u_z = 0.690\ m$

Figure 12: First mode shape of the pinched composite cylindrical shell subjected to compressive and transverse loads for progressively increasing displacements.
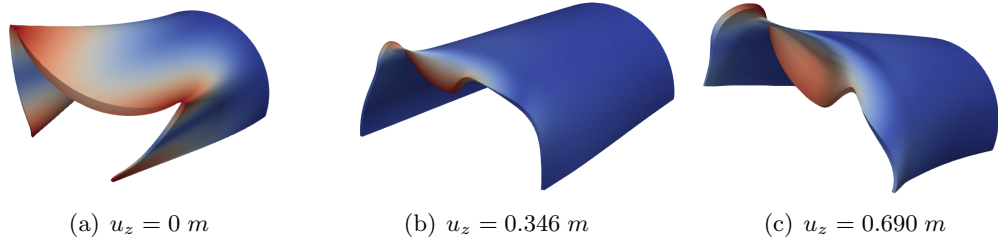

(a) $u_z = 0\ m$ (b) $u_z = 0.346\ m$ (c) $u_z = 0.690\ m$

Figure 13: Second mode shape of the pinched composite cylindrical shell subjected to compressive and transverse loads for progressively increasing displacements.

it can be observed some important phenomena, e.g. the interaction between mode 3, 4 and 5, the veering at $u_z = 0.169$ m, and the crossing at $u_z = 0.60$ m between modes 1 and 2.

4.2   Cylindrical shell undergoing snap-through

As a second assessment, a hinged cylindrical shell under a central transverse force P is considered, as illustrated in Fig. 15. This nonlinear benchmark problem is very popular due to the snapping behaviour. The isotropic cylindrical shell has: $E = 3102.75$ MPa, $\nu = 0.3$. Instead, the composite counterpart is made of a material with: $E_L = 3300$ MPa, $E_T = 1100$ MPa, $G_{LT} = 660$ MPa, $G_{TT} = 660$ MPa and $\nu_{LT} = \nu_{TT} = 0.25$. The lamination sequence considered is $[90°, 0°, 90°]$. The structure has: $L = 508$ mm, $R_\alpha = 2540$ mm, $\theta = 0.1$ rad and the thickness (h) is equal to 12.7 mm. As illustrated in Fig. 15, all nodal displacements are restrained along the hinged edges. As mentioned before, the nonlinear static behaviour of this structure was already studied in [47]. The present structure is modelled using 10×10Q9 for the in-plane mesh and 2LD3 in the z-direction for the isotropic model, whereas 4LD3 kinematics is adopted for the through-the-thickness of the composite model. Figure 16 depicts the nonlinear equilibrium curve of the hinged cylindrical shell under a central transverse force for both isotropic and composite configuration. In addition, the deformed configurations of some nonlinear conditions are illustrated in Fig. 16. Figure 17 and Table 2 provide the distribution and values of the natural frequencies of the first five and three modes, respectively. It can be noticed that the natural frequencies, illustrated in Fig. 17, gradually decreases with increasing load and, then, they rise. In particular, it is important to highlight the crossing between mode 1 and mode 2 (Fig. 17a) at $u_z = 13.10$ mm, with the consequent change of the mode shapes. Figures 18 and 19 show the evolution of these modes with respect to the quasi-static equilibrium path of the hinged isotropic structure. Moreover, MAC values are depicted in Fig. 20, showing a significant mode change for progressively increasing displacements.

In addition, for the sake of completeness, the hinged isotropic cylindrical shell subjected to compressive and transverse loads is also analyzed. In this case, the compressive-transverse load ratio is equal to 22. The equilibrium curve and the loading conditions of this further case are reported
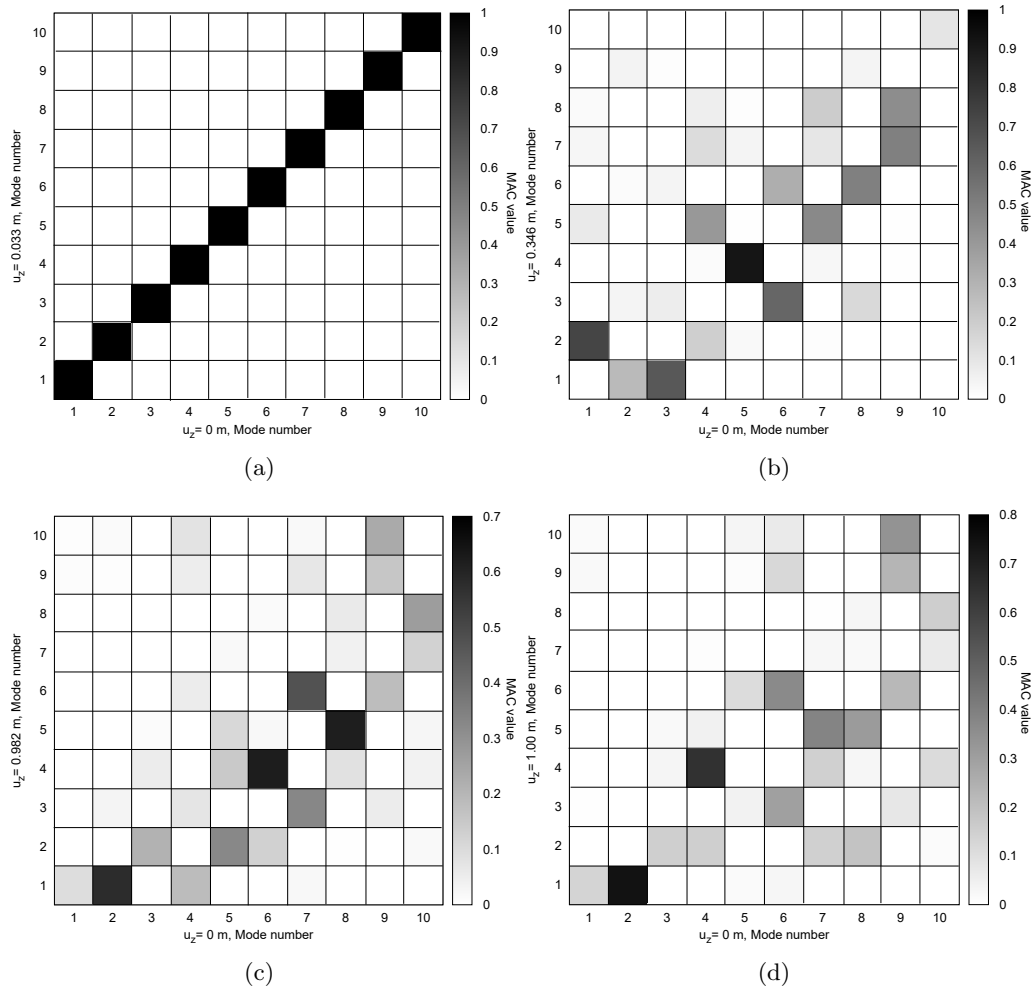
11

Figure 14: MAC values between the modes of the undeformed structure and those of the deformed structure for the pinched composite cylindrical shell subjected to compressive and transverse loads.
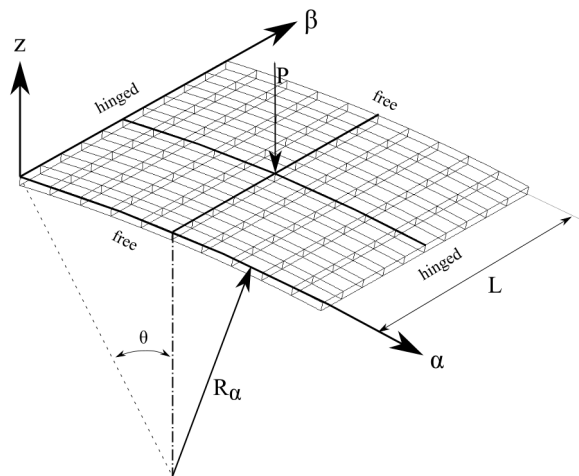

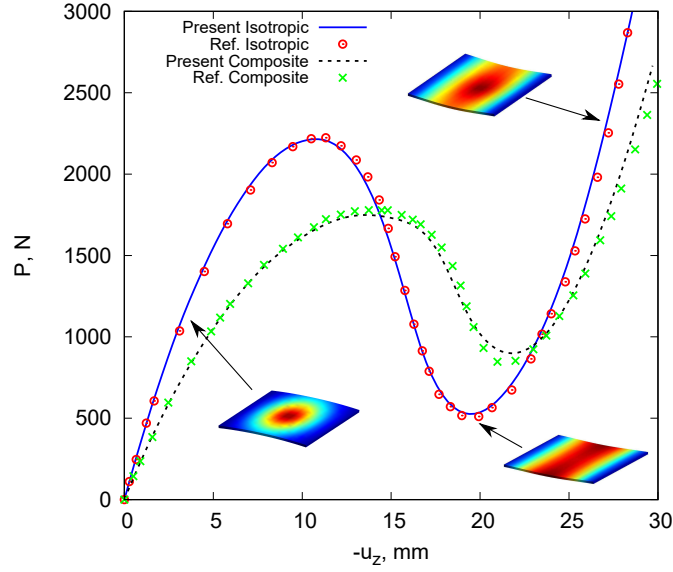Figure 15: Hinged cylindrical shell under a central transverse force.

Figure 16: Equilibrium curves of the hinged isotropic and composite cylindrical shell subjected to a central transverse force.
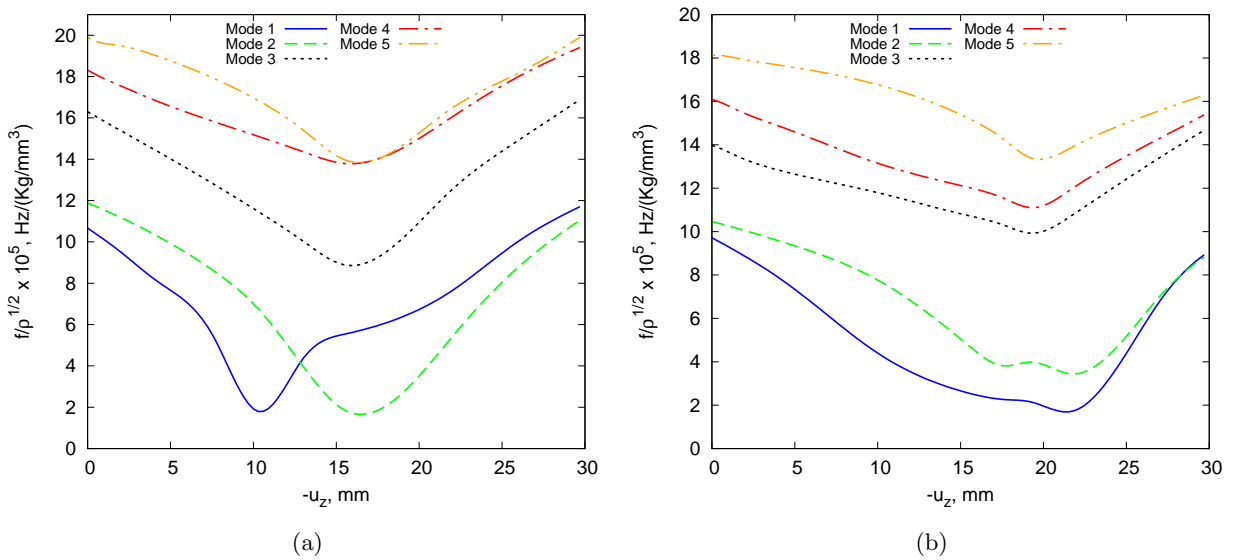

(a)

(b)

Figure 17: Natural frequencies from from modes 1 to 5. Hinged isotropic (a) and composite (b) cylindrical shell subjected to a central transverse force.

	Isotropic				Composite		
$-u_z$	$f_1/\sqrt{\rho}\times10^5$	$f_2/\sqrt{\rho}\times10^5$	$f_3/\sqrt{\rho}\times10^5$	$-u_z$	$f_1/\sqrt{\rho}\times10^5$	$f_2/\sqrt{\rho}\times10^5$	$f_3/\sqrt{\rho}\times10^5$
0.00	10.67	11.88	16.30	0.00	9.71	10.46	13.97
0.49	10.39	11.72	16.07	0.37	9.56	10.39	13.87
4.2	8.10	10.28	14.39	4.45	7.65	9.47	12.75
10.30	1.79	6.75	11.47	17.60	2.26	3.81	10.30
15.50	5.54	1.86	8.89	21.75	1.71	3.44	10.74
25.82	9.93	8.65	14.82	27.23	6.99	7.17	13.50

Table 2: Natural frequencies [Hz/(kg/mm^3)] for various transverse displacement [mm] conditions of the nonlinear analysis. Hinged isotropic and composite cylindrical shell model.

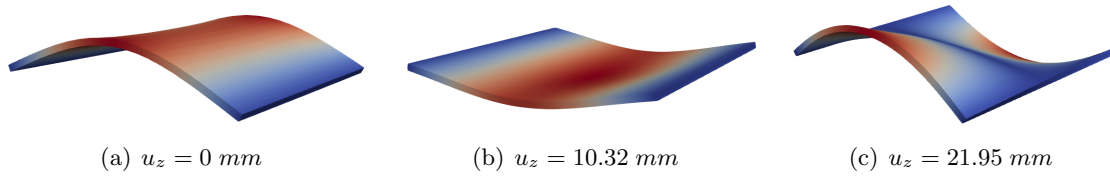(a) $u_z = 0\ mm$ (b) $u_z = 10.32\ mm$ (c) $u_z = 21.95\ mm$

Figure 18: First mode shape of the hinged isotropic cylindrical shell subjected to a transverse force for progressively increasing displacements.

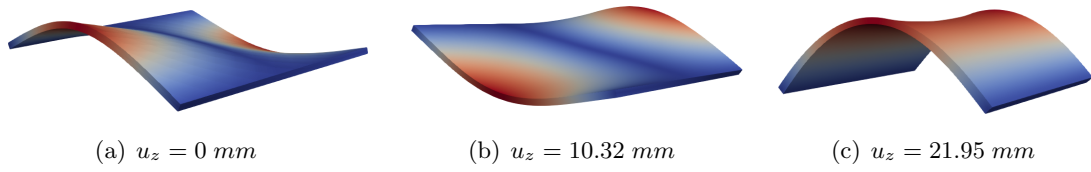(a) $u_z = 0\ mm$ (b) $u_z = 10.32\ mm$ (c) $u_z = 21.95\ mm$

Figure 19: Second mode shape of the hinged isotropic cylindrical shell subjected to a transverse force for progressively increasing displacements.
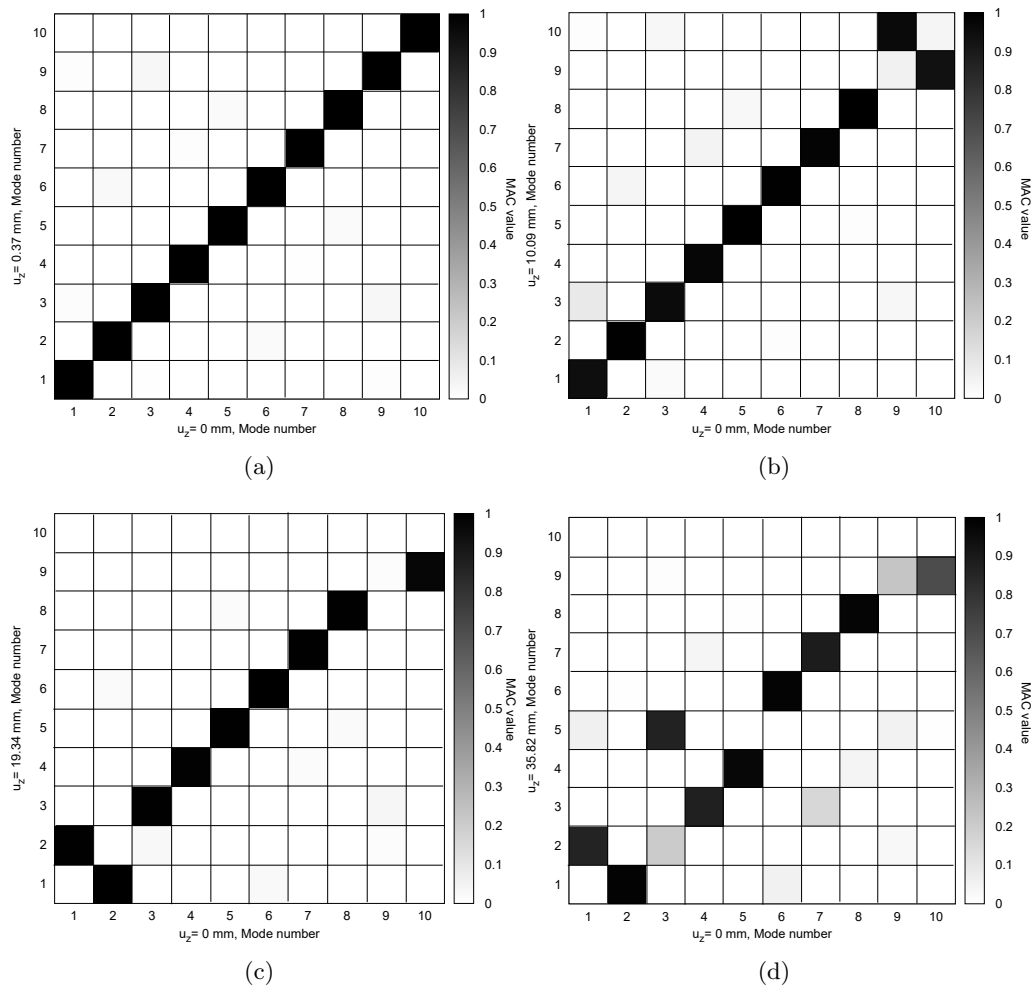

(a)   (b)

(c)   (d)

Figure 20: MAC values between the modes of the undeformed structure and those of the deformed structure for the hinged isotropic cylindrical shell.

14

in Fig. 21. Figure 22 shows the trend of the first five natural frequencies versus the transverse
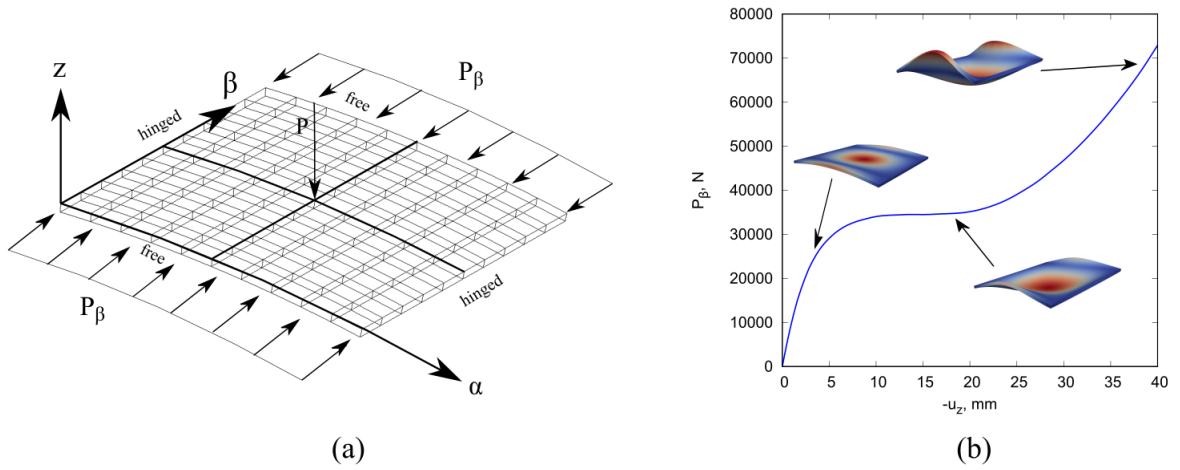

Figure 21: (a) Hinged isotropic cylindrical shell subjected to compressive and transverse loads. (b) Equilibrium curve at the transverse load point.

displacement. It can be observed that there are two important phenomena, e.g. the crossing between
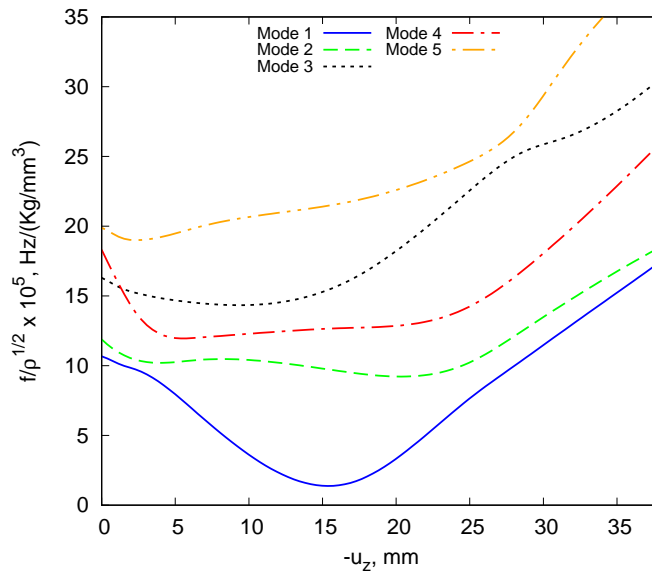

Figure 22: Natural frequencies from modes 1 to 5. Hinged isotropic cylindrical subjected to compressive and transverse loads.

mode 3 and mode 4 at $u_z = 2.39$ mm, and the veering between mode 3 and mode 5 at $u_z = 28.58$ mm. Figures 23, 24 and 25 show the evolution of the modes with respect to the quasi-static equilibrium path of the hinged isotropic cylindrical shell under compressive and transverse loads. Furthermore, the MAC graphical representations for this last case considered are illustrated in Fig. 26, showing a more significant mode change for progressively increasing displacements compared to the case with only the transverse load.

5   Conclusions

This paper has discussed natural frequency and mode change of metallic and composite shells subjected to large displacements. The analyses conducted have demonstrated that:
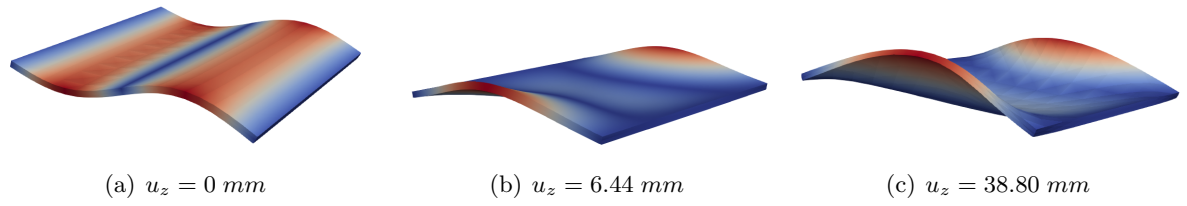
(a) $u_z = 0\ mm$ (b) $u_z = 6.44\ mm$ (c) $u_z = 38.80\ mm$

Figure 23: Third mode shape of the hinged isotropic cylindrical shell subjected to compressive and transverse loads for progressively increasing displacements.

(a) $u_z = 0\ mm$ (b) $u_z = 6.44\ mm$ (c) $u_z = 38.80\ mm$

Figure 24: Fourth mode shape of the hinged isotropic cylindrical shell subjected to compressive and transverse loads for progressively increasing displacements.

(a) $u_z = 0\ mm$ (b) $u_z = 6.44\ mm$ (c) $u_z = 38.80\ mm$

Figure 25: Fifth mode shape of the hinged isotropic cylindrical shell subjected to compressive and transverse loads for progressively increasing displacements.
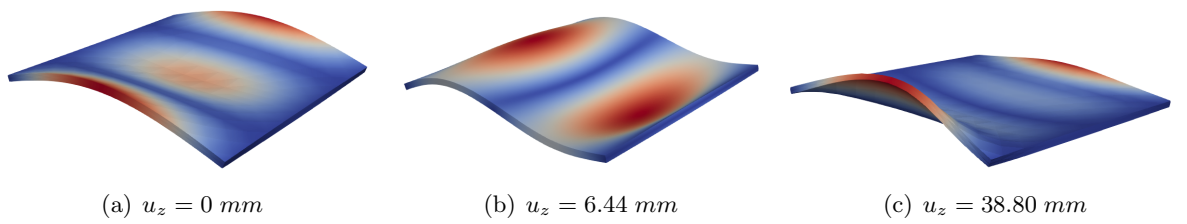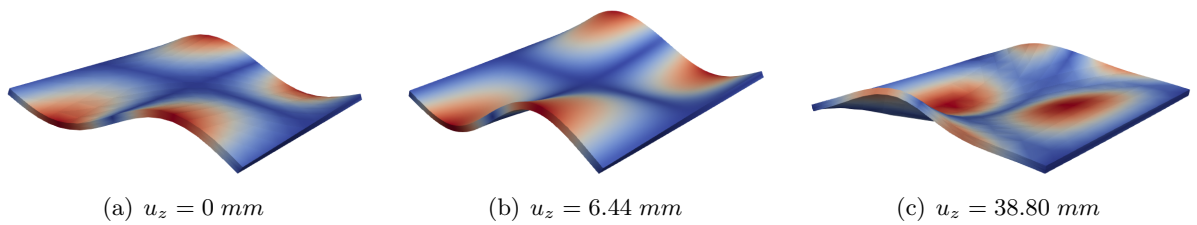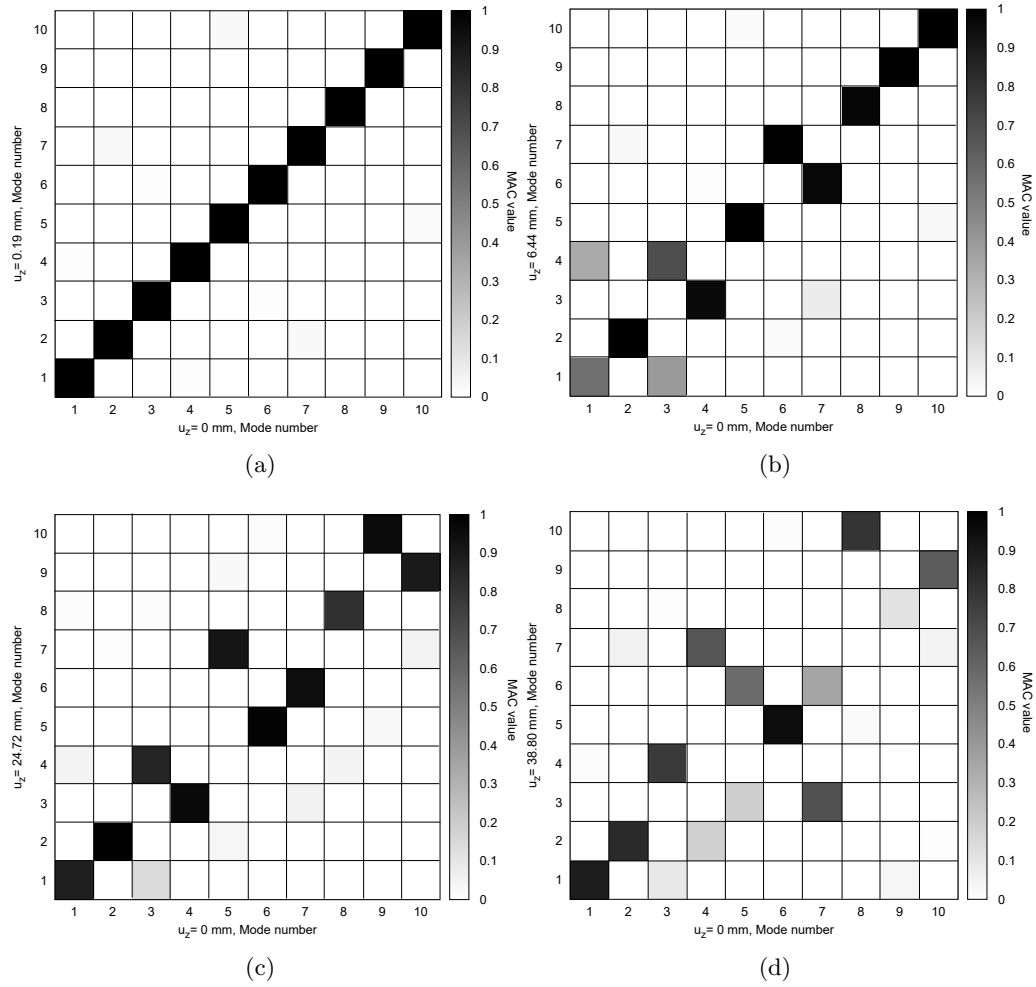
Figure 26: MAC values between the modes of the undeformed structure and those of the deformed structure for the hinged isotropic cylindrical shell subjected to compressive and transverse loads.

17

- The proposed model is able to describe accurately the nonlinear equilibrium state of composite and metallic shells;

- Natural frequencies and mode shapes may be seriously affected by pre-stress states. This is even more evident in the case of large displacement equilibrium states;

- As expected, compressive loads may cause a non-monotonic variation of the natural frequencies. Because this variation differs from mode to mode, aberrations like veering and crossing are generally observed.

- Anisotropy may be used as a means to limit nonlinear frequency and mode change. In this case, an accurate structural theory as the one proposed in this work is mandatory.

References

[1] W. Lacarbonara. *Nonlinear Structural Mechanics: theory, dynamical phenomena and modelling.* Berlin, Springer Science & Business Media, 2013.

[2] J.C. Chen and C.D. Babcock. Nonlinear vibration of cylindrical shells. *AIAA Journal*, 13(7):868–876, 1975.

[3] W.H. Wittrick and F.W. Williams. A general algorithm for computing natural frequencies of elastic structures. *The Quarterly Journal of Mechanics and Applied Mathematics*, 24(3):263–284, 1971.

[4] W.H. Wittrick and F.W. Williams. Buckling and vibration of anisotropic or isotropic plate assemblies under combined loadings. *International Journal of Mechanical Sciences*, 16(4):209–239, 1974.

[5] L.N. Virgin. *Vibration of axially-loaded structures.* Cambridge University Press, 2007.

[6] M. Amabili and M.P. Païdoussis. Review of studies on geometrically nonlinear vibrations and dynamics of circular cylindrical shells and panels, with and without fluid-structure interaction. *Applied Mechanics Reviews*, 56(4):349–381, 2003.

[7] M.A. Biot. Non-linear theory of elasticity and the linearized case for a body under initial stress. *The London, Edinburgh, and Dublin Philosophical Magazine and Journal of Science*, 27(183):468–489, 1939.

[8] G. Herrmann. *The influence of initial stress on the dynamic behavior of elastic and viscoelastic plates*, volume 16. Publ. Int. Assoc. Bridge Struct. Eng., 1956.

[9] R.W. Ogden and D.G. Roxburgh. The effect of pre-stress on the vibration and stability of elastic plates. *International Journal of Engineering Science*, 31(12):1611–1639, 1993.

[10] S.D. Akbarov. Recent investigations on dynamic problems for an elastic body with initial (residual) stresses. *International Applied Mechanics*, 43(12):1305, 2007.

[11] C.T. Sun and J.M. Whitney. Dynamic response of laminated composite plates under initial stress. *AIAA Journal*, 14(2):268–270, 1976.

[12] A.W. Leissa. *Vibration of shells*, volume 288. Scientific and Technical Information Office, National Aeronautics and Space, 1973.

[13] D.K. Shin. Large amplitude free vibration behavior of doubly curved shallow open shells with simply-supported edges. *Computers & Structures*, 62(1):35–49, 1997.

[14] H.N. Chu. Influence of large amplitudes on flexural vibrations of a thin circular cylindrical shell. *Journal of the Aerospace Sciences*, 28(8):602–609, 1961.

[15] J.L. Nowinski. Nonlinear transverse vibrations of orthotropic cylindrical shells. *AIAA Journal*, 1(3):617–620, 1963.

[16] M.D. Olson. Some experimental observations on the nonlinear vibration of cylindrical shells. *AIAA Journal*, 3(9):1775–1777, 1965.

[17] J. Mayers and B.G. Wrenn. Nonlinear free vibrations of thin, circular cylindrical shells. Technical report, Stanford Univ. CA Dept. of Aeronautics and Astronautics, 1970.

[18] D.A. Evensen and R.E. Fulton. Some studies on the nonlinear dynamic response of shell-type structures. In *Dynamic Stability of Structures*, pages 237–254. Elsevier, 1967.

[19] V.K. Singh and S.K. Panda. Nonlinear free vibration analysis of single/doubly curved composite shallow shell panels. *Thin-Walled Structures*, 85:341–349, 2014.

[20] M.H. Toorani and A.A. Lakis. Large amplitude vibrations of anisotropic cylindrical shells. *Computers & Structures*, 82(23-26):2015–2025, 2004.

[21] N. Nanda and J.N. Bandyopadhyay. Nonlinear free vibration analysis of laminated composite cylindrical shells with cutouts. *Journal of reinforced Plastics and Composites*, 26(14):1413–1427, 2007.

[22] M.M. Banerjee and J. Mazumdar. A review of methods for linear and nonlinear vibration analysis of plates and shells. *Procedia Engineering*, 144:493–503, 2016.

[23] M. Rougui, F. Moussaoui, and R. Benamar. Geometrically non-linear free and forced vibrations of simply supported circular cylindrical shells: A semi-analytical approach. *International Journal of Non-Linear Mechanics*, 42(9):1102–1115, 2007.

[24] E. Carrera, A. Pagani, and R. Augello. Effect of large displacements on the linearized vibration of composite beams. *International Journal of Non-Linear Mechanics*, 120:103390, 2020.

[25] A. Pagani, R. Augello, and E. Carrera. Frequency and mode change in the large deflection and post-buckling of compact and thin-walled beams. *Journal of Sound and Vibration*, 432:88–104, 2018.

[26] H. Abramovich, D. Govich, and A. Grunwald. Buckling prediction of panels using the Vibration Correlation Technique. *Progress in Aerospace Sciences*, 78:62–73, 2015.

[27] M.A. Arbelo, K. Kalnins, O. Ozolins, E. Skukis, S.G.P. Castro, and R. Degenhardt. Experimental and numerical estimation of buckling load on unstiffened cylindrical shells using a Vibration Correlation Technique. *Thin-Walled Structures*, 94:273–279, 2015.

[28] H. Lurie. *Lateral vibrations as related to structural stability*. PhD thesis, California Institute of Technology, 1950.

[29] E. Jansen, H. Abramovich, and R. Rolfes. The direct prediction of buckling loads of shells under axial compression using VCT-towards an upgraded approach. In *29th congress on the International Council of the Aeronutical Science*, pages 1–9, 2014.

[30] K. Kalnins, M.A. Arbelo, O. Ozolins, E. Skukis, S.G.P. Castro, and R. Degenhardt. Experimental nondestructive test for estimation of buckling load on unstiffened cylindrical shells using Vibration Correlation Technique. *Shock and Vibration*, 2015, 2015.

[31] E. Carrera, G. Giunta, and M. Petrolo. *Beam Structures: Classical and Advanced Theories.* John Wiley & Sons, 2011.

[32] E. Carrera, M. Cinefra, M. Petrolo, and E. Zappino. *Finite element analysis of structures through unified formulation.* John Wiley & Sons, 2014.

[33] E. Carrera, A. Pagani, R. Augello, and B. Wu. Popular benchmarks of nonlinear shell analysis solved by 1D and 2D CUF-based finite elements. *Mechanics of Advanced Materials and Structures*, pages 1–12, 2020.

[34] E. Carrera, M. Filippi, P.K.R. Mahato, and A. Pagani. Accurate static response of single-and multi-cell laminated box beams. *Composite Structures*, 136:372–383, 2016.

[35] M. Filippi and E. Carrera. Capabilities of 1D CUF-based models to analyse metallic/composite rotors. *Advances in AIrcraft and Spacecraft Science*, 3(1):1–14, 2016.

[36] E. Carrera and A. Pagani. Free vibration analysis of civil engineering structures by component-wise models. *Journal of Sound and Vibration*, 333(19):4597–4620, 2014.

[37] A. Pagani, M. Petrolo, G. Colonna, and E. Carrera. Dynamic response of aerospace structures by means of refined beam theories. *Aerospace Science and Technology*, 46:360–373, 2015.

[38] A. Pagani and E. Carrera. Unified formulation of geometrically nonlinear refined beam theories. *Mechanics of Advanced Materials and Structures*, 25(1):15–31, 2018.

[39] A. Pagani and E. Carrera. Large-deflection and post-buckling analyses of laminated composite beams by carrera unified formulation. *Composite Structures*, 170:40–52, 2017.

[40] B. Wu, A. Pagani, M. Filippi, W.Q. Chen, and E. Carrera. Large-deflection and post-buckling analyses of isotropic rectangular plates by Carrera Unified Formulation. *International Journal of Non-Linear Mechanics*, 116:18–31, 2019.

[41] A. Pagani, R. Augello, and E. Carrera. Virtual Vibration Correlation Technique (VCT) for nonlinear analysis of metallic and composite structures. In *ASME International Mechanical Engineering Congress and Exposition*, volume 52002. American Society of Mechanical Engineers, 2018.

[42] K.J. Bathe. *Finite Element procedure.* Prentice Hall, Upper Saddle River, New Jersey, USA, 1996.

[43] T.J.R. Hughes. *The Finite Element Method: linear static and dynamic finite element analysis.* Courier Corporation, 2012.

[44] A. Pagani and E. Carrera. Unified formulation of geometrically nonlinear refined beam theories. *Mechanics of Advanced Materials and Structures*, 25(1):15–31, 2018.

[45] M.A. Crisfield. An arc-length method including line searches and accelerations. *International Journal for Numerical Methods in Engineering*, 19(9):1269–1289, 1983.

[46] E. Carrera. A study on arc-length-type methods and their operation failures illustrated by a simple model. *Computers & Structures*, 50(2):217–229, 1994.

[47] K.Y. Sze, X.H. Liu, and S.H. Lo. Popular benchmark problems for geometric nonlinear analysis of shells. *Finite Elements in Analysis and Design*, 40:1551–1569, 2004.

[48] R.J. Allemang. The Modal Assurance Criterion - twenty years of use and abuse. *Sound and Vibration*, 37(8):14–23, 2003.

[49] M. Pastor, M.and Binda and T. Harčarik. Modal Assurance Criterion. *Procedia Engineering*, 48:543–548, 2012.